RESEARCH

UDOT Keeping Utah Moving

Utah Department of Transportation - Research Division
4501 South 2700 West - P.O. Box 148410 - SLC,UT 84114-8410

Report No. UT-24.14

EVALUATION OF METHODS FOR UDOT BRINE TANK CONDITION ASSESSMENT

Prepared For:

Utah Department of Transportation
Research & Innovation Division

Final Report
January 2024

DISCLAIMER

The authors alone are responsible for the preparation and accuracy of the information, data, analysis, discussions, recommendations, and conclusions presented herein. The contents do not necessarily reflect the views, opinions, endorsements, or policies of the Utah Department of Transportation or the U.S. Department of Transportation. The Utah Department of Transportation makes no representation or warranty of any kind, and assumes no liability therefore.

ACKNOWLEDGMENTS

The authors acknowledge the Utah Department of Transportation (UDOT) for funding this research, and the following individuals from UDOT on the Technical Advisory Committee for helping to guide the research:

- Jerry Bennett
- Kendall Draney
- Ryan Ferrin
- Stephan Foster
- Jera Irick
- Shawn Lambert
- Scott Nussbaum
- David Stevens
- Rhonda Thiele

TECHNICAL REPORT ABSTRACT

1. Report No. UT- 24.14	2. Government Accession No. N/A	3. Recipient's Catalog No. N/A
4. Title and Subtitle EVALUATION OF METHODS FOR UDOT BRINE TANK CONDITION ASSESSMENT		5. Report Date January 2024 6. Performing Organization Code N/A
7. Author(s) Moein Ramezanpour Kami, Keping Zhang, Jianli Chen, Xuan Zhu		8. Performing Organization Report No. N/A
9. Performing Organization Name and Address University of Utah Department of Civil & Environmental Engineering 110 Central Campus Drive, Suite 2000 Salt Lake City, UT 84112		10. Work Unit No. 5H090 28H 11. Contract or Grant No. 22-8115
12. Sponsoring Agency Name and Address Utah Department of Transportation 4501 South 2700 West P.O. Box 148410 Salt Lake City, UT 84114-8410		13. Type of Report & Period Covered Final Aug. 2021 to Dec. 2023 14. Sponsoring Agency Code PIC No. UT21.204

15. Supplementary Notes

Prepared in cooperation with the Utah Department of Transportation and the U.S. Department of Transportation, Federal Highway Administration

16. Abstract

UDOT manages statewide above-ground storage tanks to store brine as deicing chemicals for the winter maintenance program. The polyethylene storage tanks will age under UV light, become brittle with low temperatures, creep, and develop cracks. Structural failures of brine tanks will not only impose safety hazards to surrounding tanks and UDOT personnel but could also contaminate groundwater. While these tanks are routinely inspected to identify signs of aging and damage, current methods may not adequately capture two of the leading causes of tank failure: (a) small defects and wall thinning that can finally result in rupture and leakage, and (b) stress concentration due to inappropriate installation or uneven base. Therefore, it is essential to develop rapid inspection technologies along with guidelines as an implementable solution for UDOT's routine inspection. The recent advancement of computer vision (CV) and machine learning (ML) has been developed to be capable of automatically extracting temperature information from thermal images and evaluating deflection based on optical images. In this project, we developed accurate and efficient CV and AI algorithms to automatically identify wall thinning and measure tank wall profile/deflection by analyzing images recorded by a dual-spectrum camera. The use of the proposed technologies can potentially enable an objective full-field structural condition inspection on UDOT brine tanks, which is not available from the current practice. However, this research also establishes recommended routine inspection guidelines for UDOT brine tanks using a low-cost thermal camera rather than the dual-spectrum camera due to cost concerns.

17. Key Words Computer vision, machine learning, edge detection, thermal imaging, storage tank, condition assessment.		18. Distribution Statement Not restricted. Available through: UDOT Research & Innovation Div. 4501 South 2700 West P.O. Box 148410 Salt Lake City, UT 84114-8410 www.udot.utah.gov/go/research		23. Registrant's Seal N/A
19. Security Classification (of this report) Unclassified	20. Security Classification (of this page) Unclassified	21. No. of Pages 50	22. Price N/A	

TABLE OF CONTENTS

LIST OF FIGURES

UNIT CONVERSION FACTORS

Units used in this report and not conforming to the UDOT standard unit of measurement (U.S. Customary system) are given below with their U.S. Customary equivalents:

SI* (MODERN METRIC) CONVERSION FACTORS

APPROXIMATE CONVERSIONS TO SI UNITS

Symbol	When You Know	Multiply By	To Find	Symbol
		LENGTH		
in	inches	25.4	millimeters	mm
ft	feet	0.305	meters	m
yd	yards	0.914	meters	m
mi	miles	1.61	kilometers	km
		AREA		
in^2	square inches	645.2	square millimeters	mm^2
ft^2	square feet	0.093	square meters	m^2
yd^2	square yard	0.836	square meters	m^2
ac	acres	0.405	hectares	ha
mi^2	square miles	2.59	square kilometers	km^2
		VOLUME		
fl oz	fluid ounces	29.57	milliliters	mL
gal	gallons	3.785	liters	L
ft^3	cubic feet	0.028	cubic meters	m^3
yd^3	cubic yards	0.765	cubic meters	m^3
	NOTE: volumes greater than 1000 L shall be shown in m^3			
		MASS		
oz	ounces	28.35	grams	g
lb	pounds	0.454	kilograms	kg
T	short tons (2000 lb)	0.907	megagrams (or "metric ton")	Mg (or "t")
		TEMPERATURE (exact degrees)		
°F	Fahrenheit	5 (F-32)/9 or (F-32)/1.8	Celsius	°C
		ILLUMINATION		
fc	foot-candles	10.76	lux	lx
fl	foot-Lamberts	3.426	$candela/m^2$	cd/m^2
		FORCE and PRESSURE or STRESS		
lbf	poundforce	4.45	newtons	N
lbf/in^2	poundforce per square inch	6.89	kilopascals	kPa

APPROXIMATE CONVERSIONS FROM SI UNITS

Symbol	When You Know	Multiply By	To Find	Symbol
		LENGTH		
mm	millimeters	0.039	inches	in
m	meters	3.28	feet	ft
m	meters	1.09	yards	yd
km	kilometers	0.621	miles	mi
		AREA		
mm^2	square millimeters	0.0016	square inches	in^2
m^2	square meters	10.764	square feet	ft^2
m^2	square meters	1.195	square yards	yd^2
ha	hectares	2.47	acres	ac
km^2	square kilometers	0.386	square miles	mi^2
		VOLUME		
mL	milliliters	0.034	fluid ounces	fl oz
L	liters	0.264	gallons	gal
m^3	cubic meters	35.314	cubic feet	ft^3
m^3	cubic meters	1.307	cubic yards	yd^3
		MASS		
g	grams	0.035	ounces	oz
kg	kilograms	2.202	pounds	lb
Mg (or "t")	megagrams (or "metric ton")	1.103	short tons (2000 lb)	T
		TEMPERATURE (exact degrees)		
°C	Celsius	1.8C+32	Fahrenheit	°F
		ILLUMINATION		
lx	lux	0.0929	foot-candles	fc
cd/m^2	$candela/m^2$	0.2919	foot-Lamberts	fl
		FORCE and PRESSURE or STRESS		
N	newtons	0.225	poundforce	lbf
kPa	kilopascals	0.145	poundforce per square inch	lbf/in^2

*SI is the symbol for the International System of Units. (Adapted from FHWA report template, Revised March 2003)

LIST OF ACRONYMS

AE	Acoustic Emission
AI	Artificial Intelligence
CV	Computer Vision
EPS	Expanded polystyrene board
FE	Finite Element
FHWA	Federal Highway Administration
ML	Machine Learning
MsS	Magnetostrictive Sensor
NDE	Nondestructive Evaluation
OCR	Optical Character Recognition
SAFT	Synthetic Aperture Focusing Technique
SHM	Structural Health Monitoring
TAC	Technical Advisory Committee
TSR	Thermographic Signal Reconstruction
UDOT	Utah Department of Transportation
UGW	Ultrasonic Guided Waves

EXECUTIVE SUMMARY

UDOT manages statewide aboveground storage tanks to store brine as deicing chemicals for the winter maintenance program. The polyethylene storage tanks will age under UV light, become brittle with low temperature, creep, and develop cracks. Structural failures of brine tanks will not only impose safety hazards to surrounding tanks and UDOT personnel but could also contaminate groundwater. While these tanks are routinely inspected to identify signs of aging and damage, current methods may not adequately capture two of the leading causes of tank failure: (a) small defects and wall thinning that can finally result in rupture and leakage, and (b) stress concentration due to inappropriate installation or uneven base. Therefore, it is essential to develop rapid and low-cost inspection technologies along with guidelines as an implementable solution for UDOT's routine inspection.

First, this project reviewed existing technologies for above-ground tank inspection. The commonly used techniques include but are not limited to computer vision, robotics, ultrasonic guided waves, acoustic emission, vibrational modal analysis, and infrared thermography, among which the optical image and infrared thermography are considered as reliable ways of rapid structural condition assessment without introducing excessive cost. In addition, we have reviewed the computer vision and machine learning methods that are applicable for thermal and optical image processing for structural condition assessment of polyethylene liquid storage tanks, along with algorithms in transportation asset monitoring and inspection, including optical character recognition, edge detection, and filtering. In the past, these algorithms have been widely utilized in bridge and reinforced concrete structures inspection. Limited research has been conducted to apply the proposed approach for the applications on polyethylene liquid storage tanks.

Next, a dual-spectrum camera was used to collect data from surrogate samples in a laboratory environment. A bucket filled with water was first heated by an immersion water heater to simulate the natural heating-cooling process, where wall thinning was mimicked in three cases from the inner surface of the bucket. With the raw thermal images and the ones processed by thermographic signal reconstruction (TSR) technique, we were able to clearly detect two out of three simulated wall thickness variations. A finite element (FE) model was

developed and quantified the sensitivity of the proposed method to detect thicknesses: the high liquid temperature would result in higher temperature contrast. Also, an image processing procedure was developed to obtain a clear profile of a deformed body, which is applicable for tank wall profile/deflection measurements. The sensitivity of the proposed approach depends on the camera resolution and distance. In the laboratory environment, an accuracy of 0.1 mm can be obtained through the proposed method and algorithms.

Finally, we developed and deployed the dual-spectrum camera-based system for long-term monitoring at the UDOT Parley Springs Maintenance Shed, where both thermal and optical images were collected over four weeks during the summer of 2022. Based on the optical character recognition (OCR) analysis of thermal images, we did not identify any significant temperature anomalies that were caused by tank wall thinning, which was confirmed by the site manager. The developed OCR algorithm can support temperature prediction of a 98% correlation with the actual temperature. Moreover, the brine tank profile was extracted through our computer vision algorithms, which can support a deflection accuracy of 1 mm. No significant profile and deflection variations were identified through the four-week period. The team also performed site inspection using a handheld thermal camera. While there were no active leakages, the collected thermal images effortlessly highlighted water marks from previous water leakages. Thus, the proposed approach can support sufficient sensitivity (tens of °C) for detecting brine leakages due to structural failures.

The developed dual-spectrum camera-based technology in this project delivers an accurate, efficient, and automated approach to collect and analyze thermal and optical imagery. Moreover, due to cost concerns, the research team recommends using the low-cost thermal camera for routine inspection of UDOT brine tanks rather than the dual-spectrum camera. The research results would benefit Utah by supporting a safer operation of UDOT brine storage tanks, preventing safety hazards, and minimizing environmental impact from UDOT brine tank failures.

1.0 INTRODUCTION

1.1 Problem Statement

UDOT manages statewide aboveground storage tanks to store brine as deicing chemicals for the winter maintenance program. The polyethylene storage tanks will age under UV light, become brittle with low temperature, creep, and develop cracks. Structural failures of brine tanks will not only impose safety hazards to surrounding tanks and UDOT personnel but could also contaminate groundwater. While these tanks are routinely inspected to identify signs of aging and damage, current methods may not adequately capture two of the leading causes of tank failure: (a) small defects and wall thinning that can finally result in rupture and leakage, and (b) stress concentration due to inappropriate installation or uneven base. Therefore, it is essential to develop rapid inspection technologies along with guidelines as an implementable solution for UDOT's routine inspection.

First, the team will develop an infrared thermographic measurement system to detect wall thinning of brine tanks. A structural defect can lead to nonuniform thermal diffusion property, and thereby, a local hot or cool spot, which can be easily detected by a full-field infrared thermographic measurement. With the natural heating and cooling cycles, a temperature contrast led by a structural defect can be identified and monitored. Second, the team will develop a low-cost rapid inspection technology to identify stress concentration due to installation error or uneven base by detecting and monitoring any discrepancies between a tank profile. The presence of tank wall deformation and a significant change in wall deflection over time can serve as indications of tank structural failure. The inspection involves capturing optical images and performing computer vision (CV) techniques to extract and monitor the tank profile. This technology can support a rapid and robust profile inspection using machine learning algorithms. Last, the team will work with UDOT to understand how the developed technology can be integrated with the current UDOT brine tank inspection practice.

1.2 Objectives

The primary project objective is to (a) develop inspection technologies addressing the leading causes of above-ground storage tank failure, and (b) establish guidelines for UDOT brine tank inspection.

1.3 Scope

The project consists of six main research tasks (listed below), i.e., developing a data collection prototype, developing computer vision and machine learning algorithms for processing thermal and optical images, identifying tank wall thinning through analyzing thermal images, quantifying the tank wall profile/deflections based on optical images, evaluating system performance, and developing a brine tank inspection manual. The six specific tasks are listed below:

Task 1: Literature review: Review the literature regarding the latest technologies for above-ground tank inspection.

Task 2: Design and develop data collection prototype.

Task 3: Work with UDOT on data collection.

Task 4: Develop and evaluate computer vision and machine learning algorithms for data processing.

Task 5: Work with UDOT on developing a brine tank inspection manual.

Task 6: Project report preparation: Prepare the final project report.

1.4 Outline of Report

The remaining report is structured as follows. Chapter 2 reviews the sensing technologies for inspecting liquid storage tanks, including the applications of thermal imaging and machine learning. Chapter 3 introduces the measurement systems and computer vision algorithms developed based on laboratory tests. The results and performance of the developed approaches

for wall thinning detection and tank wall deflection measurement are quantified. Chapter 4 describes the field data collection and analysis at the UDOT Parley Springs Maintenance Shed. Finally, Chapter 5 summarizes the key findings and recommendations for future work.

2.0 LITERATURE REVIEW

2.1 Overview

Infrastructure plays a vital role in modern society by supporting essential services such as transportation, energy, and communication. As a result, ensuring the safety and reliability of infrastructure is critical for maintaining the well-being and productivity of the community. Nondestructive evaluation (NDE) and structural health monitoring (SHM) can support detecting potential defects and damages in structures before they become a safety hazard (Mishra et al., 2022). In the context of liquid storage tank infrastructure, vertical and horizontal tanks are widely used for storing and distributing water. The leading causes of tank failure include the stress concentration due to inappropriate installation, or uneven base and small defects and wall thinning that can finally result in rupture and leakage. One of the factors that can affect the structural condition of liquid storage tanks is temperature, which can cause thermal expansion and lead to deflection and distortion of the tank structure (Batista-Abreu and Godoy, 2013). A range of NDE techniques have been proposed to detect and monitor these potential sources of damage (Rochman and Suhariyanto, 2021). Bhadauria et al. (2007) presented a study on the in-situ performance testing of deteriorating water tanks to assess their durability. They conducted a comprehensive study that involved visual inspection, ultrasonic pulse velocity, rebound hammer test, core extraction for strength evaluation, and chloride content analysis in assessing the corrosion potential. They also highlighted the need for regular inspection and maintenance of liquid storage tanks to ensure their durability and safe operation. Amiri and Sabbagh-Yazdi discussed the use of ambient vibration tests as a nondestructive method to evaluate tall liquid storage tanks' natural frequencies and mode shapes (Amiri and Sabbagh-Yazdi, 2011). They compared the results of the ambient vibration tests with those obtained from finite element (FE) models of the tanks and found a good agreement between the two. They observed the potential of ambient vibration tests as a reliable and cost-effective method for assessing the dynamic behavior of liquid storage tanks, particularly for existing tanks where access to destructive testing may be limited. However, each method has limitations in terms of accuracy and reliability, particularly when it comes to detecting early-stage damage. In this chapter, we

reviewed major nondestructive evaluation technologies that have been applied on the inspection of liquid storage tanks.

2.2 Computer Vision and Robotics

Video cameras are the most used sensors when it comes to above-ground storage tank inspection, and they are usually companions with the deployment of robotics. A common defect-detection algorithm using computer vision is composed of the following steps: image pre-processing, image segmentation, and morphological operation, as detailed by Giergiel et al. (2012). The flowchart, as shown in Figure 2-1 (left, below), demonstrates the typical image processing algorithms. The input image is first filtered by an average filter, and local binarization to distinguish dark regions is carried out, followed by image segmentation. After the segmentation stage, a morphological operation would be implemented to highlight the crack geometry and orientation. Such an image processing procedure is generally effective in identifying cracks in metals and concrete structures. For polyethylene tanks, defect detection is usually challenging since the defect appearance is generally different from cracks and spalling.

On the other hand, there has been extensive research on the development of robotic systems to perform visual or other inspection measurements. An example design can be found in Figure 2-1 (right, below). The whole robot is designed based on a piped framework which provides lightness and stiffness. The piped modules can be easily modified, optimized, and fabricated. The piped framework allows easy connections. Tracks allow the robot to move, especially on the tank bottom. Helical drive with optional ballast tanks enables free motions in liquid. The whole robot is supplied and controlled via cables from a safe place outside of storage tanks. The second unit is a robotized probe attached to the main robot by the wire. This robot is responsible for the inspection and diagnostics of the walls. It can search for any visual damages using such a detection method as checking carbonatization, looking for corrosion of metal structures, and searching for macro cracks on the walls. There is a need that the robot should operate underwater to examine the bottom of the tank and tank walls. Most existing inspection robots are designed for metal tanks – they are equipped with magnetic wheels or magnetic caterpillar tracks to move on vertical walls (Hein et al., 1992; Schempf et al., 1995; Longo et al., 2004; Kalra et al., 2006; and Moniri et al., 2015). They are usually designed to look for corrosion

of metal elements or damages in welded connections between metal structures. The general problem is that in most cases of robotic inspection procedures, tanks should be empty prior to the deployment. Because such procedures could last over one month, the tank will be unavailable for service during this extended period.

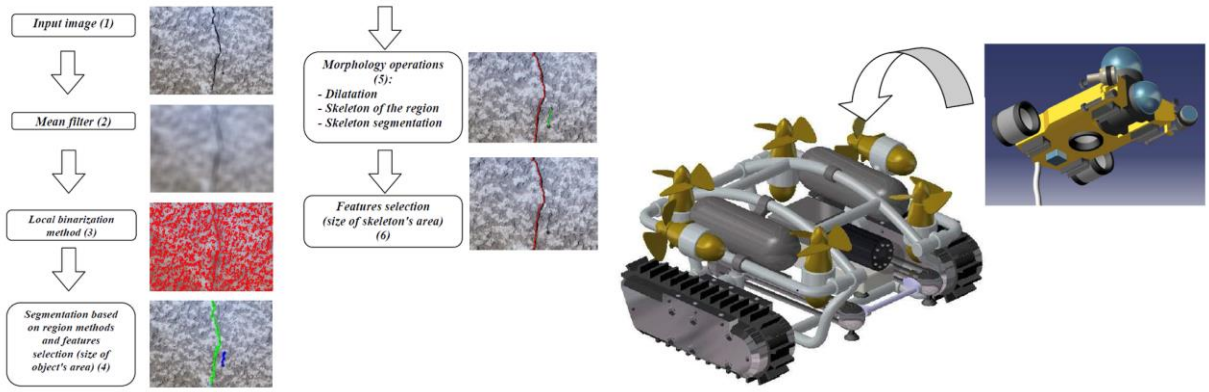

Figure 2-1 The scheme of the implemented wall-damage detection algorithm (left) and the model of inspection mobile robotized system (right). (Giergiel et al., 2012)

2.3 Ultrasonic Guided Waves

Ultrasonic guided waves (UGW) propagating in waveguide structures are generally governed by the confinement of geometries, including plate, shell, bar, pipeline, and rail. When wavelengths are comparable with waveguide geometries, one can model the wave propagation as ultrasonic guided waves. This is a non-invasive and economically viable means of assessing structural integrity conditions. A drastic difference between the ultrasonic bulk and guided waves is that ultrasonic bulk waves feature constant wave velocities, while guided waves are mostly dispersive. The dispersion nature makes ultrasonic guided waves more difficult to model or work with. However, guided waves propagate along the waveguide structures and, thereby, experience less geometric attenuation compared to bulk waves. For example, ultrasonic guided waves can propagate over 10 meters in rails without significant attenuations.

Lowe et al. (2017) adopted ultrasonic guided waves to focus on assessing the structural integrity condition of above-ground storage tanks. They attached d33 and d31 types of ultrasonic transducers to the tank wall to induce ultrasonic disturbance with a center frequency of 45 kHz at

the tank floor. Both the symmetric and asymmetric Lamb modes were promoted. They modeled guided wave propagation through numerical simulation and validated the models on a 4.1-meter diameter tank. Their study demonstrated that the d31 type transducers bonded to the tank wall could be used to introduce ultrasonic guided waves and assess the structural integrity condition of tank floors, as shown in Figure 2-2. Their parametric study illustrated that there is a 7.4 dB signal-to-noise ratio improvement at 45 kHz for the guided wave excitation on the tank wall using d31 transducers. These parameters are generally governed by the geometry of the piezoelectric elements and the thickness of the tank floor. Similar technology can be implemented for tank-wall-thinning inspection. However, it requires a sophisticated modeling tool to understand the wave modes and potentially a dense sensor array for defect detection.

Puchot et al. (2014) developed a screening technique for above-ground storage tanks that uses a magnetostrictive sensor (MsS) guided wave technology and a Synthetic Aperture Focusing Technique (SAFT) to map the condition of a tank floor from the outside of the tank. They performed preliminary tests on a mockup setup resembling the tank floor and wall. Data collection was conducted by accessing the tank exterior surface and scanning with the MsS probe. Their study demonstrated that the developed inspection technique could effectively identify the presence of pitting corrosion and local corrosion in the tank floor. It is notable that the magnetostrictive sensors are only applicable to ferromagnetic materials and not to polyethylene materials. Moreover, the data acquisition system for SAFT is usually sophisticated and expensive. However, the idea of using guided waves incorporated with the SAFT imaging system is feasible for corrosion detection in storage tank structures.

2.4 Acoustic Emission

Acoustic emission (AE) monitoring systems provide effective monitoring for corrosion and fracture processes via detecting bulk or guided waves generated by the sudden releases of stored strain energy. Some important signal characteristics measured by AE sensors include event hit rate, energy, waveform shape parameters, and event central frequency. When properly deployed and evaluated, AE data can be used to estimate the locations and occurrence times of the AE source (cracking site). As shown in Figure 2-3 (left), AE has been extensively studied to detect the corrosion of the tank bottom, which has been the main cause of metallic tank leakage

(Murakaimi et al., 2007; Gang et al., 2010; Lin et al., 2010; Mejia et al., 2010). Compared with the other measurement approaches, the AE technology needs long-term monitoring but does not require a service interruption to empty the tank. The existence of corrosion in the tank bottom can be identified by AE techniques based on the amount and density of AE events. However, 3D localization for corrosions of the tank bottom could be challenging. Considering the condition of wave propagation, waveform and frequency spectra of AE signals would be difficult to evaluate due to the presence of noises, which could resemble subtle corrosion signals. Such a noisy testing environment can seriously influence the accuracy with which corrosion locations can be identified.

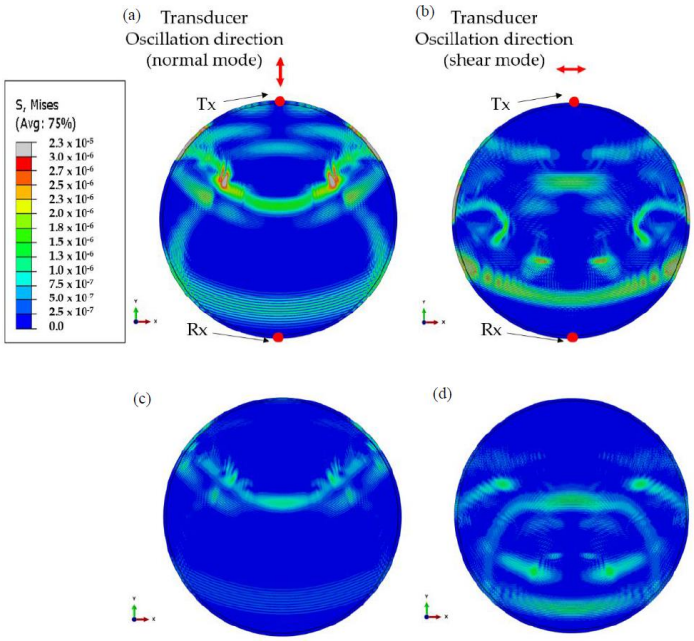

Figure 2-2 FEA results of ultrasonic guided wave with a PZT bonded on the annual chime applied (a) normal stress; (b) shear stress. A PZT bonded on the tank wall applied (c) normal stress; and (d) shear stress. (Lowe et al., 2017)

To address such challenges, Lin et al. (2010) deployed guard sensors to shield inside-tank noise signals during AE monitoring, which facilitated extracting characteristics of AE signals from tank-bottom corrosion areas. Such an advancement enabled the localization and classification of corrosion events occurring on the tank bottom. Data-driven models have also been studied for AE monitoring. Murakami et al. (2007) investigated both the bulk wave and guided wave for corrosion damage localization on the tank bottom. They developed a neural

network (NN) model to understand the relationship between the differences in the time-of-flight from four AE sensors and the coordinate of AE source locations. The data-driven model would significantly reduce the complexity of the velocity model considering possible variations of boundary and support conditions. While this study demonstrated robust prediction performance, we speculate that the pencil-breaking tests adopted for model training might not represent the subtle corrosion events and, thereby, could have limited implications for real-world applications.

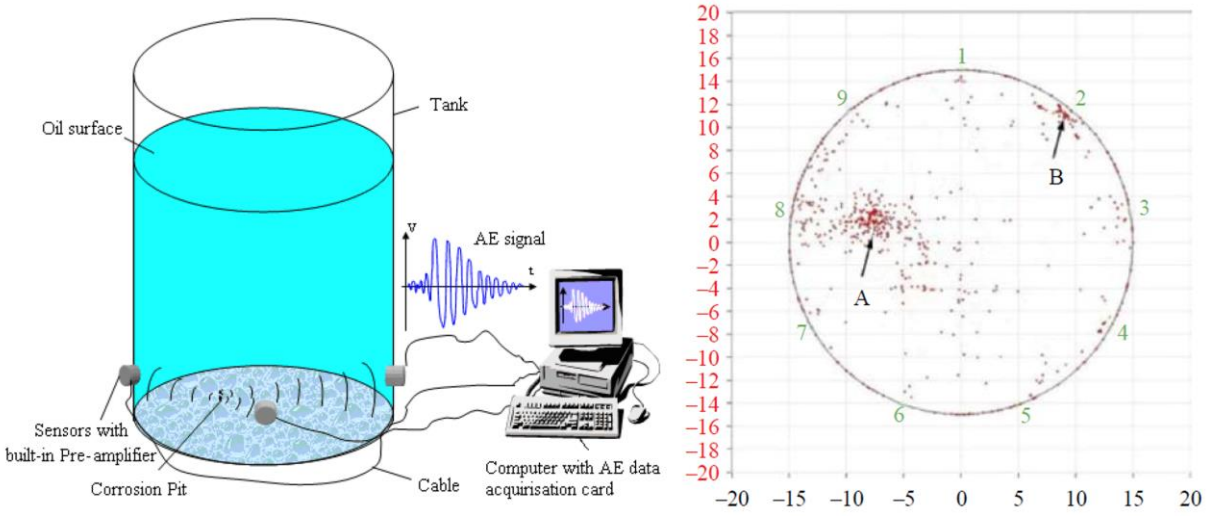

Figure 2-3 The principle of AE monitoring for above-ground storage tanks (left) and AE localization of the corrosion at the tank floor (right). (Lin et al., 2010)

2.5 Thermal-Optical Imaging and Machine Learning

Thermal and optical cameras offer a comprehensive and economic approach to assessing the structural condition of liquid storage tanks, as they can detect both surface and internal defects caused by temperature changes and deformation. Thermal cameras have been widely used to monitor temperature changes in various structures, including liquid storage tanks. Behravan et al. (2021) conducted a laboratory study where they used two nondestructive testing techniques, namely thermography and ultrasonic testing, to evaluate the condition of polyethylene liquid storage tanks. They subjected the tanks to different loading conditions, including thermal cycling and static loading, and analyzed the thermographic and ultrasonic data to assess the tanks' condition. They concluded that the use of thermal cameras offers a highly

accurate and reliable approach for detecting potential defects caused by temperature changes in polyethylene liquid storage tanks. With the growing interest of utilizing machine learning (ML) for condition assessment and monitoring, it can potentially enhance the accuracy and reliability of NDE methods, leading to more efficient and effective monitoring of infrastructure health. As one of these ML techniques, Optical Character Recognition (OCR) methods can extract and analyze temperature information from thermal images captured by cameras, providing further insights into the structural condition of polyethylene liquid storage tanks. By continuously monitoring the temperature of a tank over a period of time, it is possible to detect anomalies corresponding to the thinning tank wall.

Furthermore, researchers have suggested employing high-resolution cameras to monitor the structural stability of liquid storage tanks, who usually scrutinize the images captured by such cameras to identify any deformation or deflection, as they may indicate possible structural impairment. Similarly, Pan et al. (2022) suggested the use of high-resolution cameras and an adaptive mask for remote deflection detection of long-span bridges. Edge detection algorithms are used to identify changes in bridge deflection under varying conditions. The research demonstrates the efficacy of edge detection as a useful tool for detecting changes in bridge deflection and highlights the potential of the proposed method as a practical and cost-effective approach for monitoring the health of long-span bridges. Consequently, the use of image processing techniques, such as edge detection, may increase the accuracy and sensitivity of the detection process and provide a complete method for monitoring the deflection of polyethylene liquid storage tanks.

3.0 LABORATORY TESTS

3.1 Overview

In this chapter, experimental investigations were conducted to understand the effectiveness of the proposed approaches in a controlled environment. First, we collected thermal images on a heated surrogate liquid storage tank. Wall thickness was modified to quantify the performance. Moreover, a finite element model was developed to understand the heat diffusion process of typical polyethylene liquid storage tanks. Second, optical images of undeformed and deformed samples were collected, and we developed the image processing algorithm to quantify deflections. By tracking the deflections, we can identify potentials of local stress concentrations in polyethylene liquid storage tanks.

3.2 Laboratory Thermal Image Collection and Analysis

3.2.1 Test Setup

A bucket filled with water was used as a surrogate sample. The water level in the bucket was 14 inches, and it was heated by an immersion water heater, which simulates the natural heating-cooling process. To mimic wall thinning of polyethylene liquid storage tanks, three simulated defects were attached at the inner surface of the bucket: a piece of duct tape with a thickness of 0.018 inch, a piece of double-sided tape with a thickness of 0.076 inch, and a piece of foam as shown in Figure 3-1.

Two tests were conducted: (i) the duct-taped and double-sided taped sample was heated from 26.9°C to 45°C, and we turned off the water heater until it cooled down to 36.9°C, as shown in Figure 3-2(a); (ii) the foam-attached sample was heated from 20.3°C to 50°C, and we turned off the water heater until it cooled down to 46.9°C, as shown in Figure 3-2(b). Throughout the heating and cooling cycle, a dual spectrum IR camera system was used to monitor the surface temperature of the bucket. Moreover, the ground truth of bucket temperature was measured by a thermocouple.

(a) (b) (c)

Figure 3-1 Three types of defects simulated using (a) duct tape, (b) double-sided tape, (c) foam.

(a) (b)

Figure 3-2 Test setup (a) duct tape and double-sided tape sample, (b) foam sample.

3.2.2 Test Results and Analysis

Figure 3-3 shows the temperature response of the duct-taped and double-sided taped sample. From the raw and adjusted thermal images during the cooling cycle, a local temperature

variation that appears as a hot spot was observed at the double-sided-taped location. The double-sided-taped area featured a higher temperature contrast (temperature difference compared to the other areas). The reason is that the thick tape can obstruct more flow of heat. However, the duct-taped location is less obvious, where the adjusted thermal image shows a slight temperature contrast.

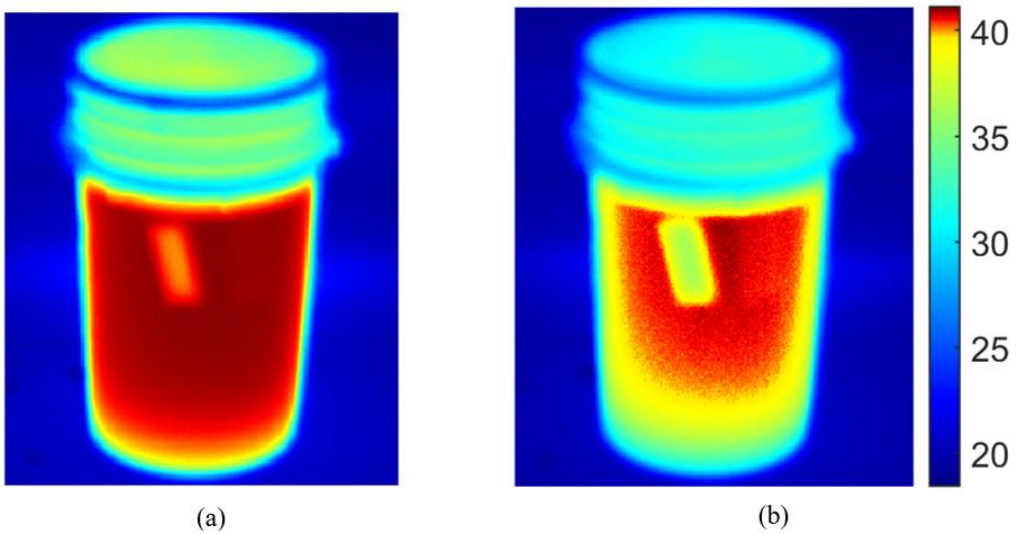

Figure 3-3 Thermal images of double-sided tape and duct tape sample during cooling down cycle: (a) raw image, (b) adjusted image

To enhance the performance of using thermal images for defect detection, the thermographic signal reconstruction (TSR) technique was implemented for defect enhancement. In TSR, the logarithmic temperature response of each pixel is fit to a first-order polynomial. Then, derivatives of the logarithmic signal, calculated with respect to logarithmic time, were constructed for amplifying defect deviation from the normal temperature. Figure 3-4(a) shows the time evolution of the first and second derivative of the double-sided-taped area with a pixel location of (152, 154). The amplitude peaks at ln (2) s in the second derivate, which generally indicates changes in the heat diffusion process. The corresponding thermal image is shown in Figure 3-4(b). While the double-sided-taped area was highlighted, the duct-taped location in the second derivate image was not retrieved as expected. The reason can be attributed to the fact that the TRS signal processing may only be suitable for pulse, step thermal excitation, and not for continuous thermal excitation.

Figure 3-5 shows the results using foam as the defect. From both the heating and cooling cycle, the raw thermal image can clearly show the contour of the foam and duct tape.

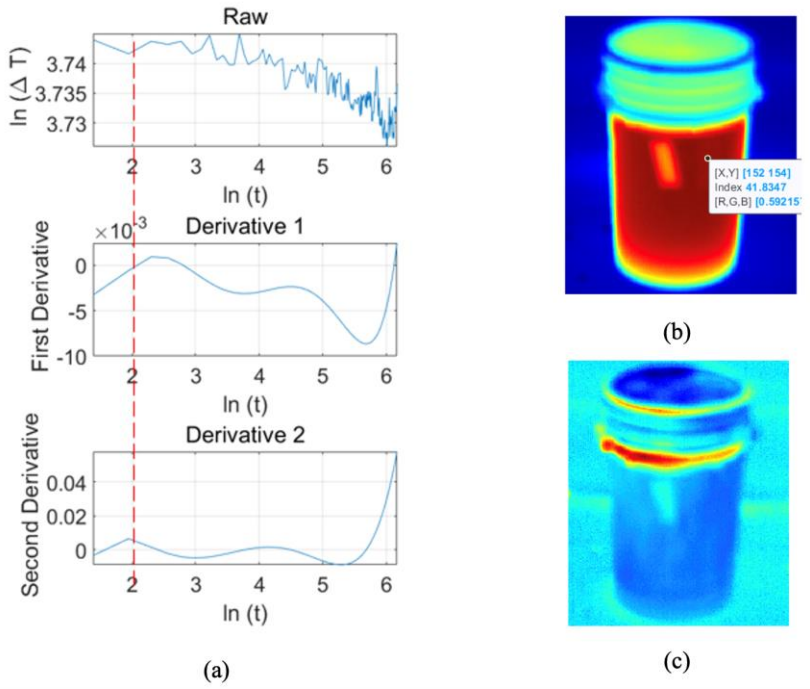

Figure 3-4 TSR result: (a) temperature evolution, first derivative and second derivative at duct tape with pixel location (152, 154), (b) thermal raw image at time ln (2) s, (c) second derivative image at time ln (2) s.

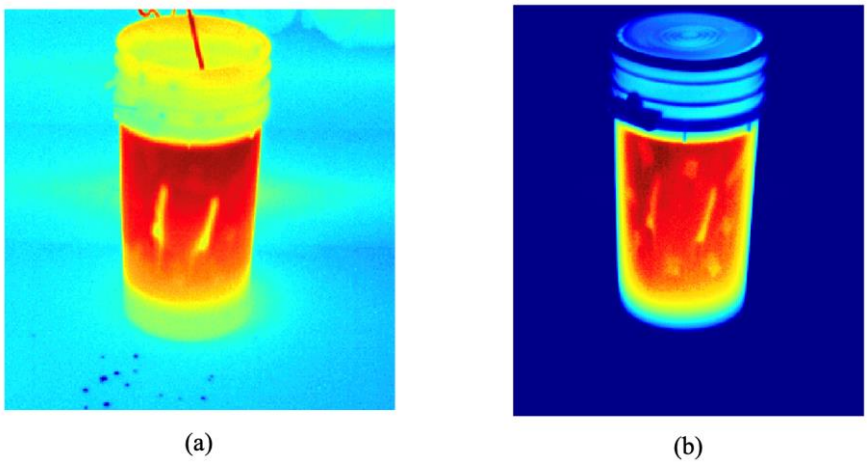

Figure 3-5 Thermal raw image of foam sample: (a) heating-up cycle, (b) cooling-down cycle.

3.2.3 Numerical Simulation

A finite element model was developed by COMSOL software to study the effects of defect thickness on temperature distribution. As shown in Figure 3-6, the bucket wall thickness is 2 mm. The bucket and defect materials were considered as expanded polystyrene board (EPS) with a thermal conductivity of 0.05 W/(m·K). A 2D plane-strain model was adopted to simulate heat transfer along the wall thickness direction. The initial temperature of the entire domain is set as 293.15 K. Since the outer surface encounters air, and the inner surface encounters hot water, the effect was considered by applying the convective heat transfer coefficient. We took two points' temperature on the outside of the wall to present the temperature contrast ΔT. One is at the defect location with the temperature T_1, the other is at nominal surface with the temperature T_2. The bucket and defect were meshed with triangular elements using a mesh size of 1 mm. A stationary study was performed.

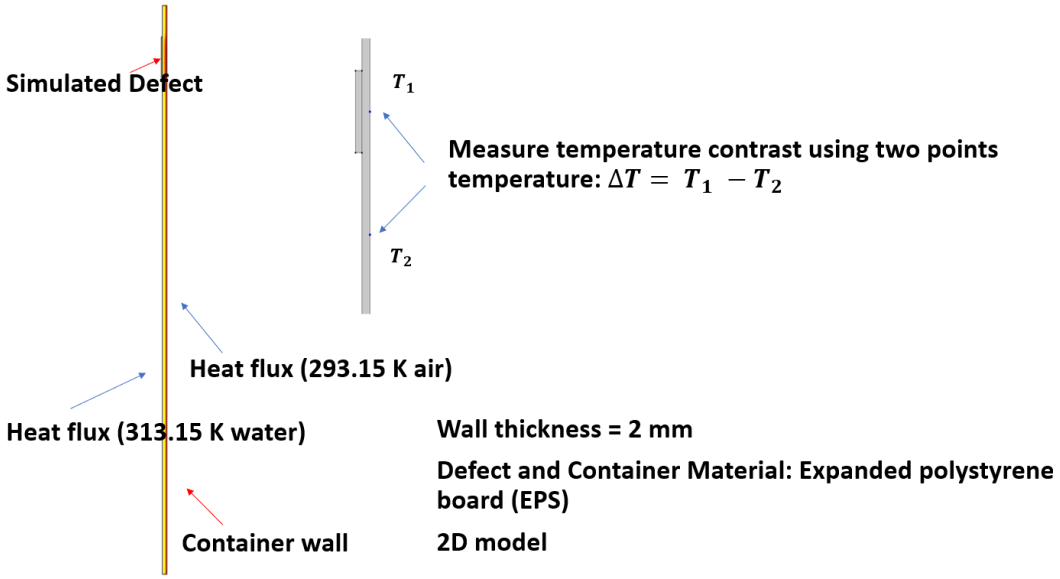

Figure 3-6 Simulation setup.

A parametric study for defect thickness effect was conducted within the range 0.5 mm to 2 mm. Temperature contrast (abs ΔT) increases with the defect thickness as shown in Figure 3-7(a) and (b), which demonstrates that the thicker defect can obstruct more flow of heat. Temperature measured at the defect location is lower than the nominal surface. Simulation results agree well with the lab test observation. The more the thickness change, the larger

temperature contrasts that we can observe. Furthermore, the higher the temperature of container water, the defect would cause higher temperature contrast at the outside of the bucket wall.

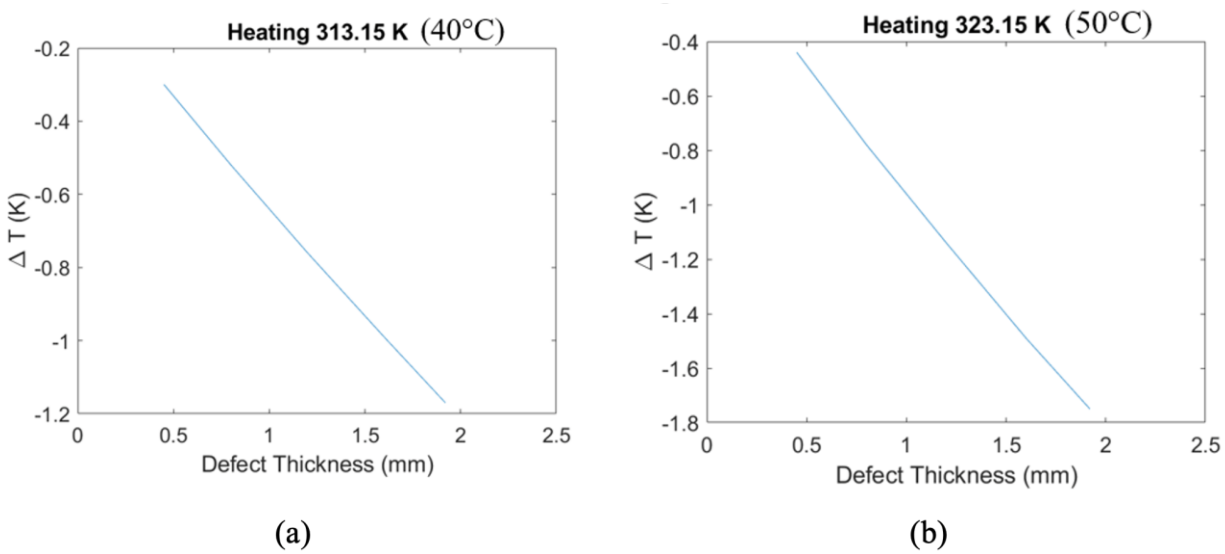

(a) (b)

Figure 3-7 The effect of defect thickness on temperature contrast with (a) 40°C water and (b) 50°C water.

3.3 Laboratory Optical Image Collection and Analysis

3.3.1 Test Setup

In order to remotely measure the deflection of a tank wall, we developed image processing techniques on a surrogate sample and evaluated its feasibility. We used an optical camera to capture images of a foam cube at its undeformed and deformed states, as shown in Figure 3-8.

3.3.2 Test Results and Analysis

Edge detection techniques, as depicted in Figure 3-9, were applied to identify the edges of the prototype and hence its deformation. To improve accuracy, the following steps were implemented: The image was cropped to focus on the appropriate section of the sample, a Gaussian blur filter was applied to eliminate noise, thresholding was used to enhance the edge clarity, and erosion was utilized as a morphological method to refine the edge thickness.

Furthermore, in order to evaluate the displacement of the edge on the left side of the foam sample after loading, the center of the white pixels was computed for each row of the image, as shown in Figure 3-10.

Figure 3-8 The image captured using a Sony optical camera of (a) an undeformed foam cube and (b) a deformed foam cube.

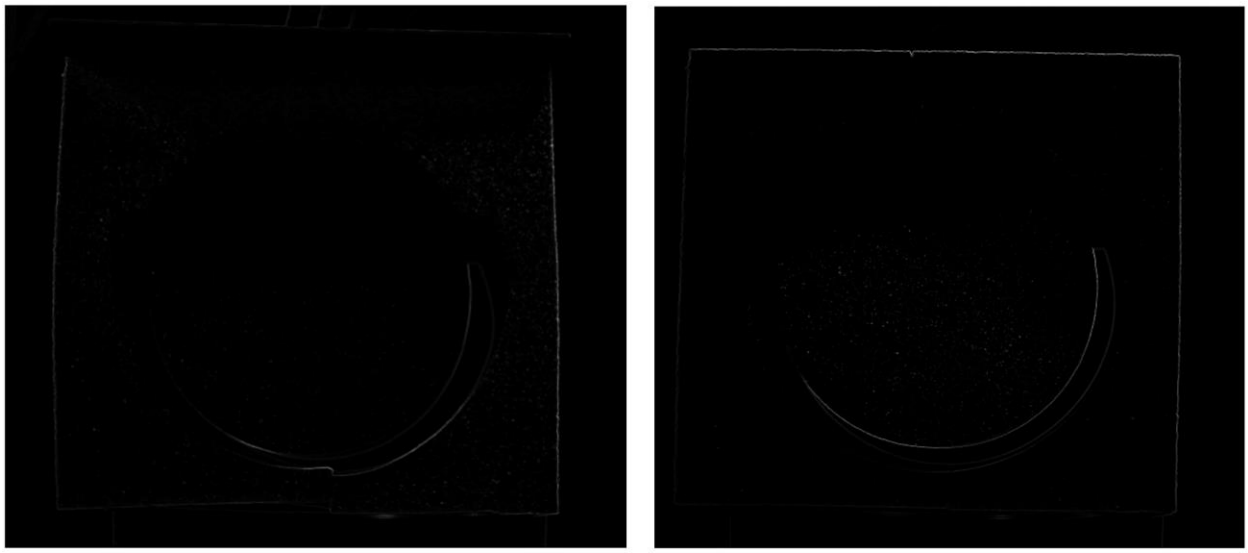

Figure 3-9 The edges detected by the Sobel operator on an undistorted foam cube (left) and the distorted foam cube (right).

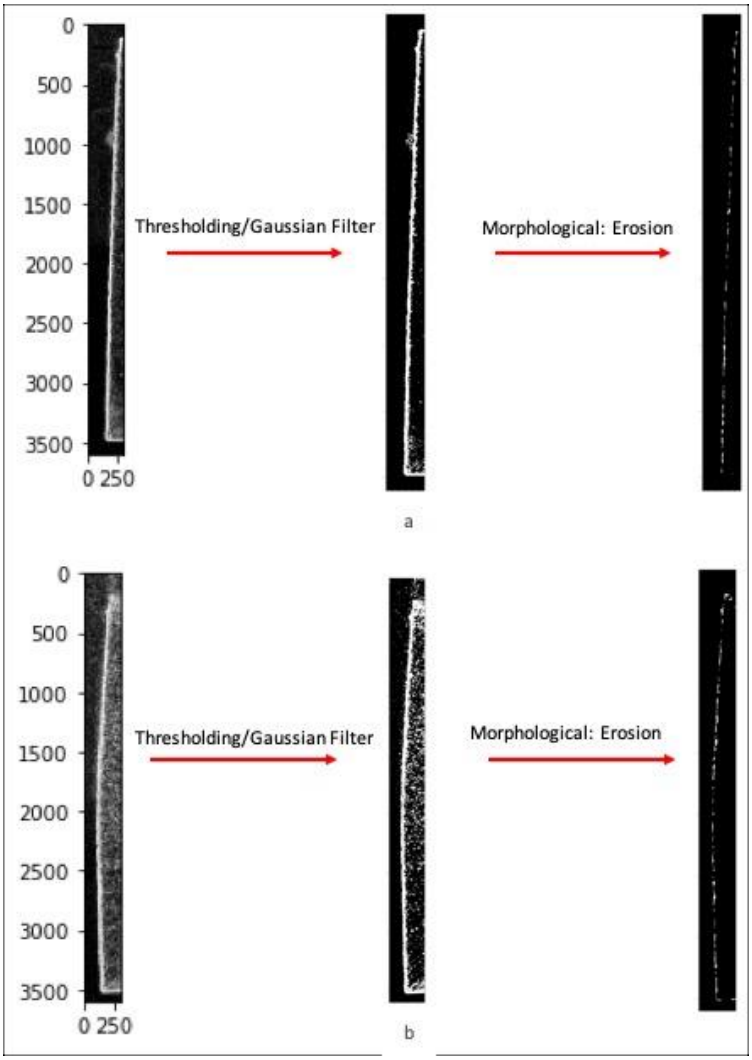

Figure 3-10 Image processing to obtain a clear edge of (a) an undeformed foam cube, and (b) a deformed foam cube.

The primary objective of this study was to monitor wall tank deformations using nondestructive evaluation techniques. The deflection of the surrogate sample was determined using an optical camera with the edge detection image processing technique. The precision of the optical camera for measuring small deformations was evaluated by computing the deformation of the prototype sample using Sobel edge detection. Figure 3-11 demonstrates steps to determine the maximum displacement of the left edge of the deformed foam sample, which measures 95 pixels.

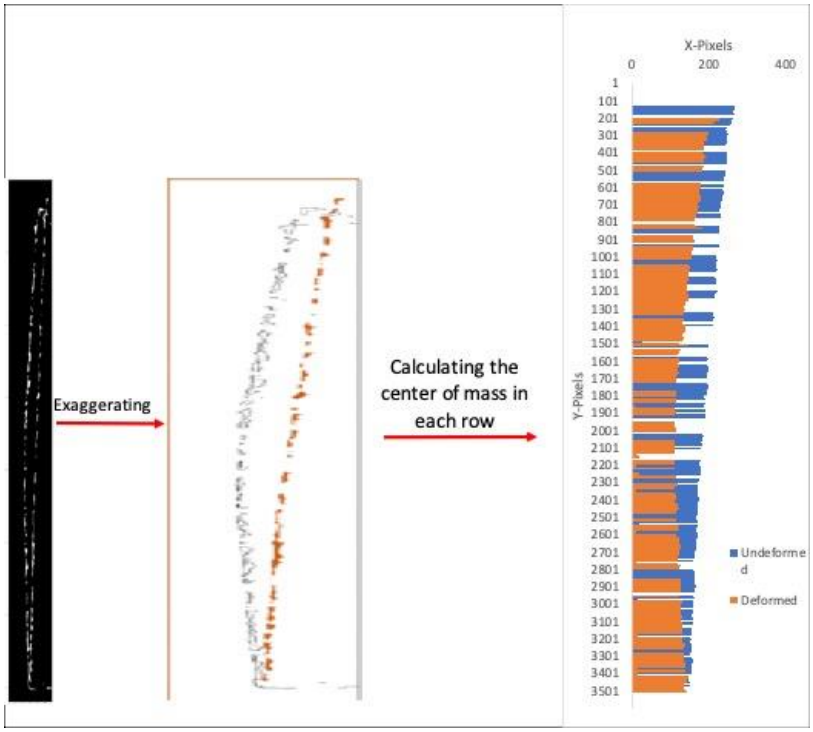

Figure 3-11 Steps to obtain the maximum displacement of the left side of deformed foam in pixels.

Four points with 1 cm intervals were selected in the image, as shown in Figure 3-12. By extracting their coordinates, the achieved accuracy for the deformation is approximately 0.1 mm, which is a testament to the performance of the proposed approaches.

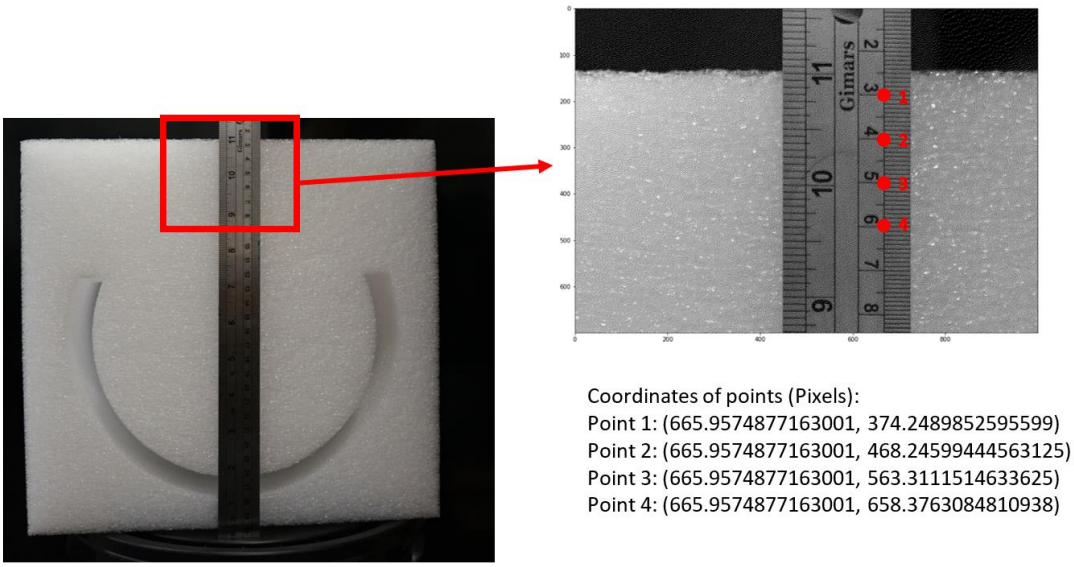

Figure 3-12 Selection of four points and extracting the coordinates of points.

3.4 Summary

In this chapter, we developed nondestructive methods to determine variations of wall thickness based on thermal images and quantify wall deflections using optical imagery. These approaches, along with processing algorithms, were developed and evaluated, and their performance is satisfactory in a laboratory environment.

4.0 FIELD TESTS

4.1 Overview

In this chapter, we conducted data collection and analysis based on the developed techniques at a UDOT site. First, we performed long-term monitoring using a dual-spectrum camera targeting brine tanks at the UDOT Parley Springs Maintenance Shed. Both thermal and optical images were collected over four weeks during the summer of 2022. Second, we performed multiple site visits and collected data using a low-cost handheld device. The collected data are analyzed based on techniques we developed in the previous chapter.

4.2 Long-Term UDOT Brine Tank Monitoring

The long-term brine tank monitoring focuses on tracking the maximum temperature and variations of tank wall deflections over a four-week period.

4.2.1 Test Setup

The team conducted data collection at the UDOT Parley Springs Maintenance Shed from August 4th to September 1st, 2022, for which a Google Maps view is shown in Figure 4-1. There are two groups of brine tanks without any reported leakages, as shown in Figure 4-2. During the period when inspection was favorable (summer months), the brine tanks were filled with stormwater. A long-term monitoring system was developed and deployed at the maintenance shed close to the tanks. Considering the cost and limitations, the designed system was positioned toward one group of tanks in the first two weeks and then positioned toward the other group of tanks in the second two weeks.

The InfiRay IRS-FB462A dual-spectrum bullet camera, with an operating temperature ranging from -40 to 70℃, was selected for its endurance in the severe field environment. Its uncooled microbolometers cover a spectral range of 8 to 14 μm and support infrared imaging with a resolution of 640 by 512 and an accuracy of ±2℃. The field of view of the infrared imager is 22° by 18°. Moreover, the optical lens of the camera provides a resolution of 1920 by

1080 with a wider FOV compared to its infrared imager. This network camera simultaneously streams optical and thermal images with an interval of 1/25s, which are directly transferred and stored in a rugged laptop. The dual-spectrum camera was attached to an extendable pole on the trailer via a customized fixture, which was lifted to approximately 10 ft (~3 m). The portable trailer continuously powered the data collection system with sets of batteries and solar panels, as shown in Figure 4-3. The recorded optical and thermal images were regularly saved and transferred for further processing, as shown in Figure 4-4. The aim of this field test is to understand the temperature range of brine tanks in the Parley Springs site and evaluate the feasibility of wall thinning and deflection detection based on our field observations.

Figure 4-1 Google Maps view of UDOT brine tanks at the Parley Springs Maintenance Shed.

Figure 4-2 Two groups of UDOT brine tanks at the Parley Springs Maintenance Shed.

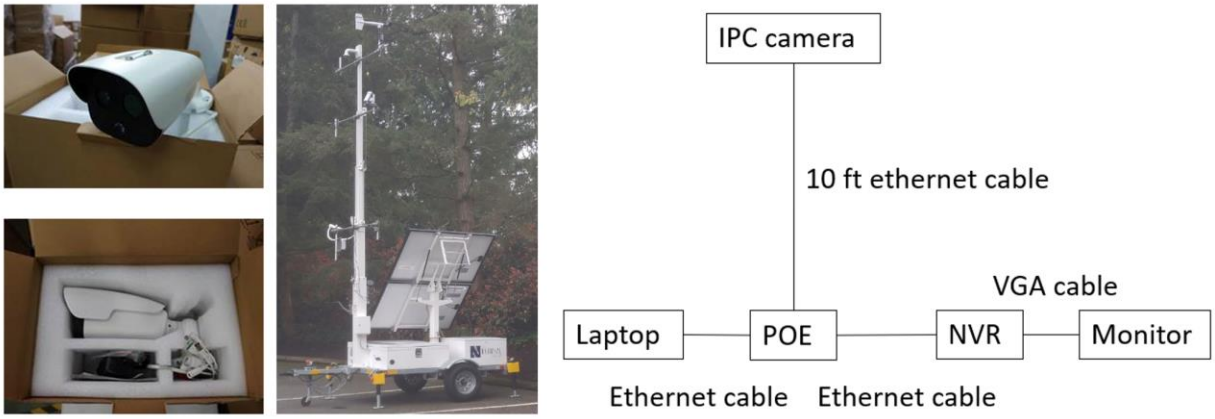

Figure 4-3 InfiRay IRS-FB462A dual-spectrum bullet camera and portable trailer (left); and the system design for automated data collection (right).

Figure 4-4 Dual-spectrum camera mounted on the portable trailer (left) and typical data collected at the UDOT Parley Springs Maintenance Shed.

4.2.2 Data Analysis on Thermal Images

To determine the minimum, maximum, and average temperatures of the UDOT brine tanks, we used OCR to convert symbols in the images to specific numbers. The OCR method was applied in MATLAB, where we preprocessed the images by filtering and thresholding them before using the OCR function to extract the temperature values. We trained the computer with existing number symbols; then, the OCR function was applied to the original thermal image to extract temperature numbers. The OCR approach was used to convert symbols in the images to specific numbers for the extraction of the minimum, maximum, and average temperature of the water tank and the temperature of the center of the water tank. Figure 4-5 demonstrates the minimum, average, and maximum temperature, and temperature of the center of the image over 14 days with 2-hour intervals. It is notable that some minimum temperature values are below freezing point, which is mainly caused by passing vehicles on the highway in the background. Considering the temperature readings at the center of the field of view and the maximum temperatures, it will suffice to support wall-thickness change detection using the developed algorithm. No significant temperature variations were observed.

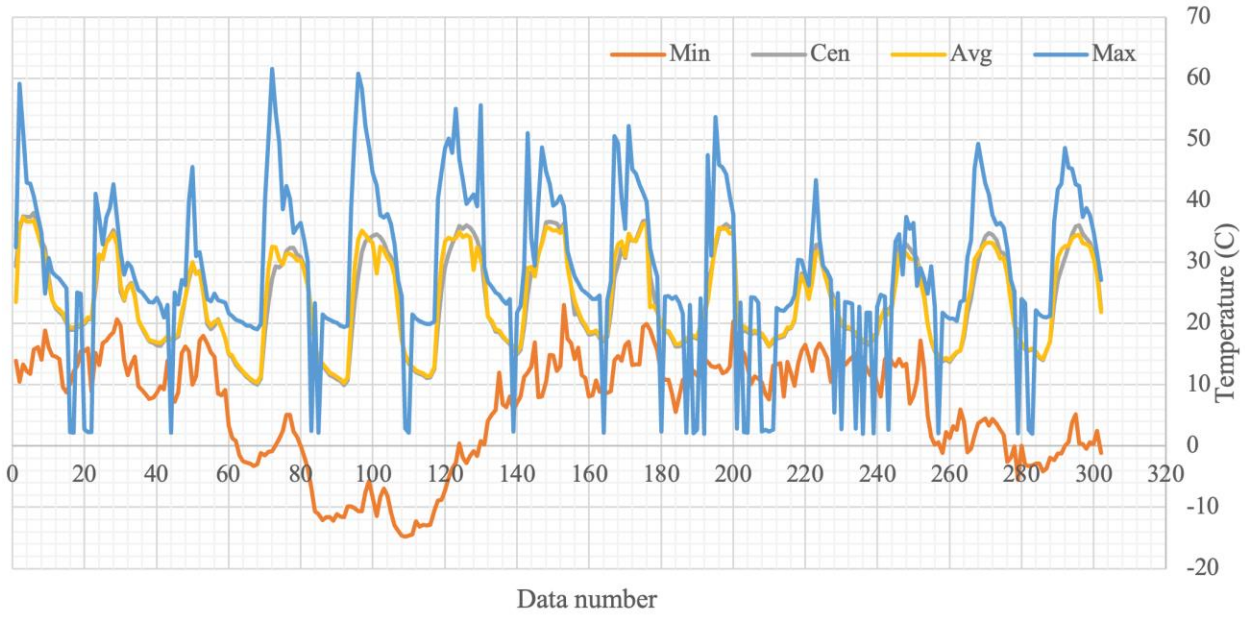

Figure 4-5 The minimum, average, and maximum temperature, and the temperature of the center of the image over time.

Comparing the actual and extracted temperature indicates that the OCR approach was able to determine the temperature of the center of the water tank with a 98 percent correlation with the actual temperature, as shown in Figure 4-6, underscoring the effectiveness of OCR as a method for temperature extraction from thermal images. There are a few cases where the extracted temperatures are off, which mainly resulted from errors of the OCR algorithm.

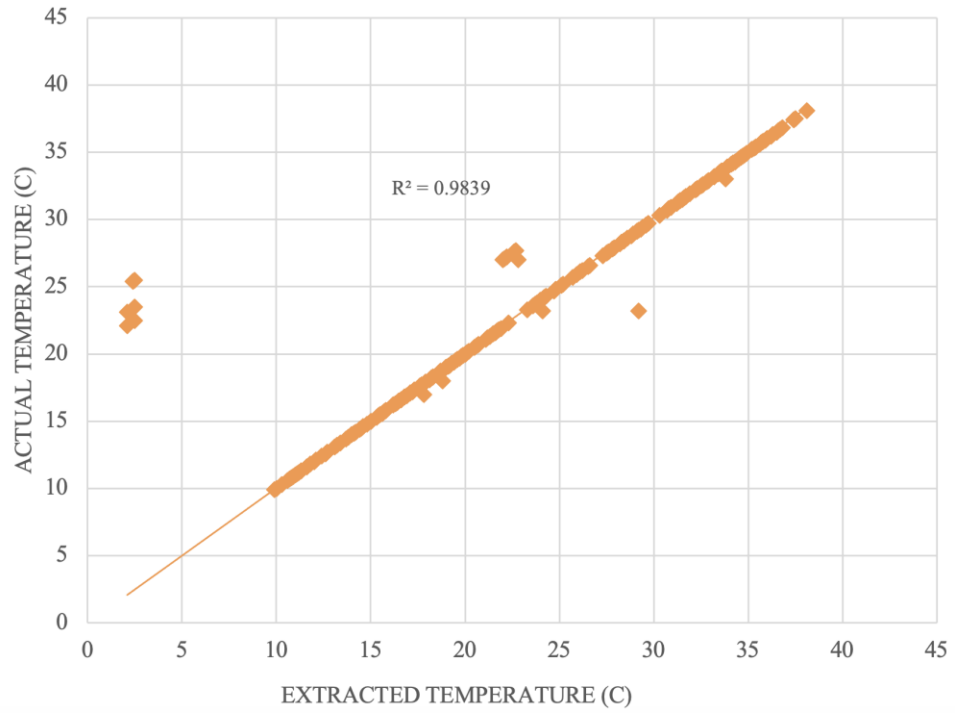

Figure 4-6 Comparison of the actual and extracted temperature.

4.2.3 Data Analysis on Optical Images

Once we determined the accuracy of the optical camera in finding deformation in the prototype, we applied the same technique to the UDOT brine tank with high contrast in temperature, where we expect to see large deflection due to the thermal effects. We used the optical camera to capture images of the water tank and applied the same image processing techniques as with the prototype to detect the deflection of the water tank. The deformation of the water tank was determined by following a procedure similar to that used for the surrogate sample, which involved measuring the displacement of the edges. The edge detection results are shown in Figure 4-7.

To understand the accuracy of the image processing algorithm for deformation calculation, the same algorithm was applied to the foam sample and extended to the water tank in the field. The findings reveal that when the camera is positioned 10 meters away from the water tank, the accuracy achieved for the deformation calculation is 1 mm, which is a reasonable precision considering the camera's distance from the UDOT brine tanks, as shown in Figure 4-8.

The obtained data from the low-resolution dual-spectrum camera posed a challenge in accurately determining the deformation of the water tank. Figure 4-9 shows that despite the almost 30℃ temperature difference between optical images, the deflections were consistent without a significant variation due to the thermal expansion. Therefore, it is recommended to use high-resolution cameras for such measurements.

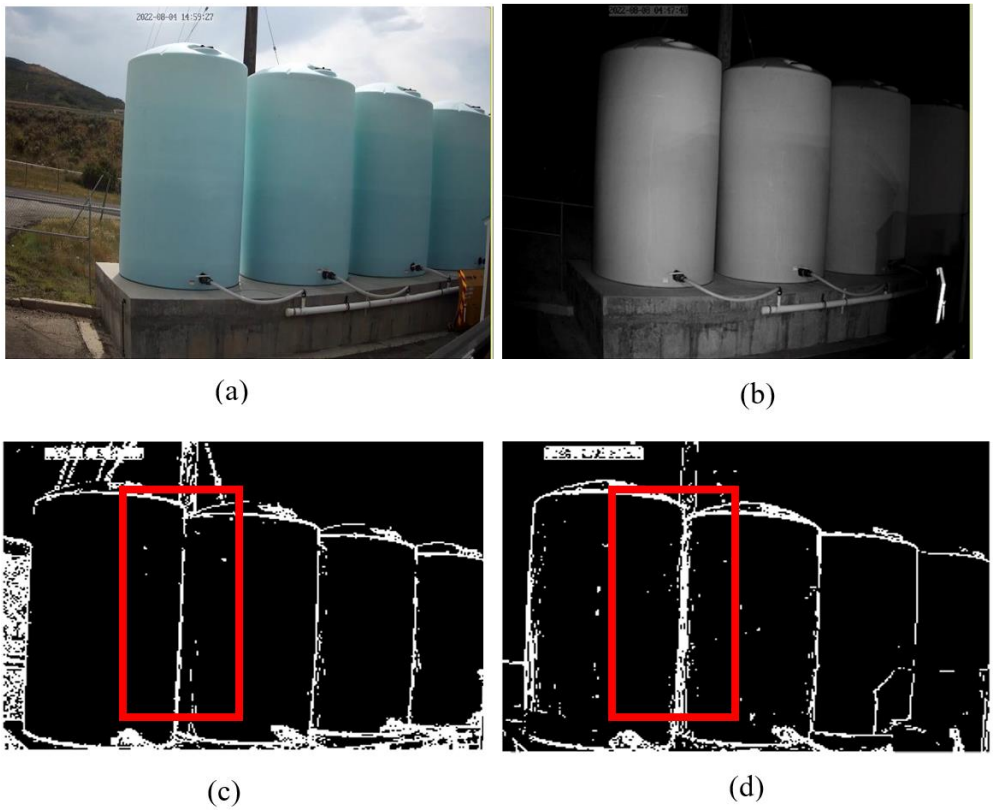

Figure 4-7 (a) Image of the water tank with center temperature of 38.1℃, (b) image of the water tank with center temperature of 9.9℃, (c) edge detection by the Sobel operator on with center temperature of 38.1℃, and (d) edge detection by the Sobel operator on with center temperature of 9.9℃

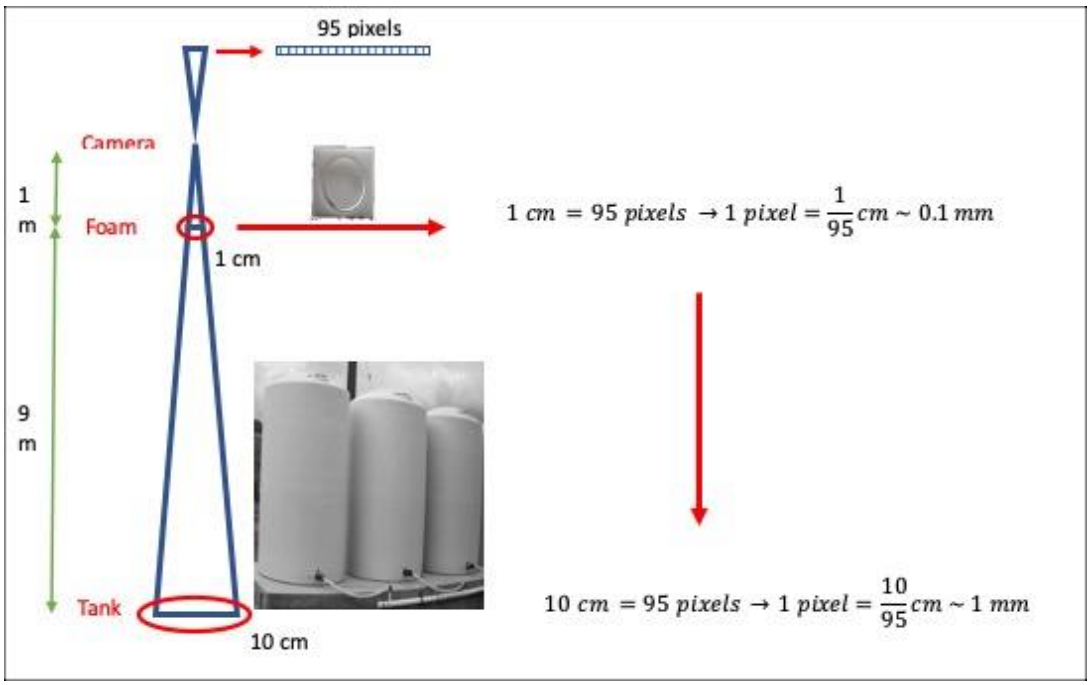

Figure 4-8 Calculate the field of view of the camera and calculation of the accuracy of the optical camera to detect deformation in the field.

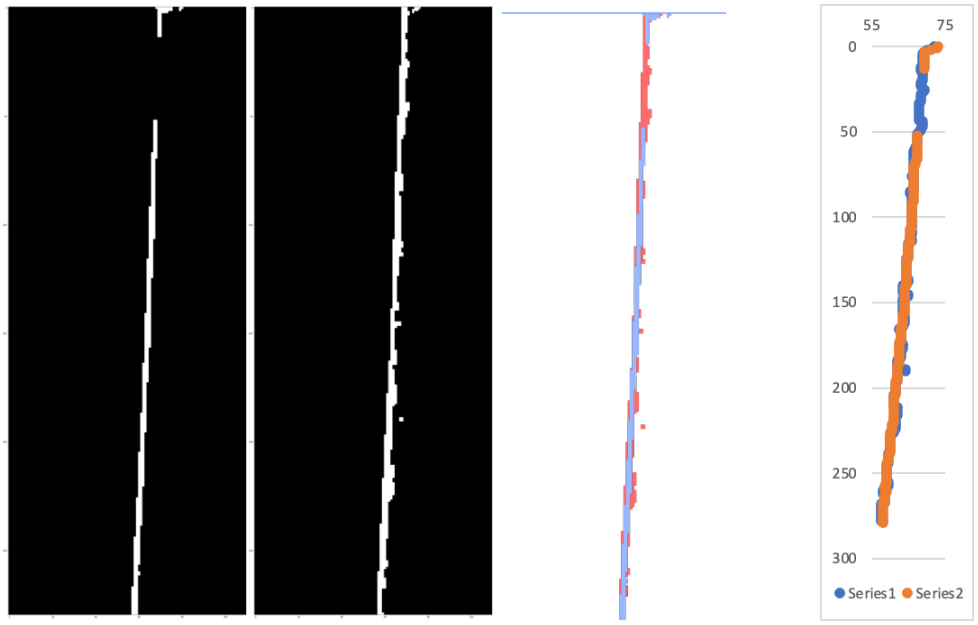

Figure 4-9 Steps to obtain the displacement of a specific side of water tanks in pixels.

4.3 Site Inspection Using a Handheld Thermal Camera

For UDOT inspection practice, we visited the site with a handheld thermal camera in the summer of 2023. There were no significant temperature variations during the time of visit, and we focused on the lower half of the brine tanks. The handheld thermal camera is the FLIR ONE Pro, which is perfect for finding water damage. This FLIR ONE Pro camera offers 4 times the native resolution of the FLIR ONE Pro LT, for sharper image clarity that's further enhanced by the revolutionary FLIR VividIR™. Measured temperatures can go up to 400°C (752°F) with a sensitivity that detects temperature differences down to 70 mK. The FLIR ONE Pro camera was attached to a personal iPhone for data collection. Our inspection did not identify any leakages at the time of visit, which was confirmed by the site manager. However, the thermal images were able to highlight the marks from previous leakages due to errors during pipe installation. The optical and corresponding thermal images of four (out of 20) brine tanks, where water marks were identified, are shown in Figure 4-10. It is notable that the temperature difference can be as high as tens of °C even without the presence of active leakage. Thus, the proposed thermal camera can support sufficient sensitivity for detecting water leakages due to structural failures. Based on these findings, we established the "UDOT Brine Tank Inspection Manual" and attached it in Appendix A.

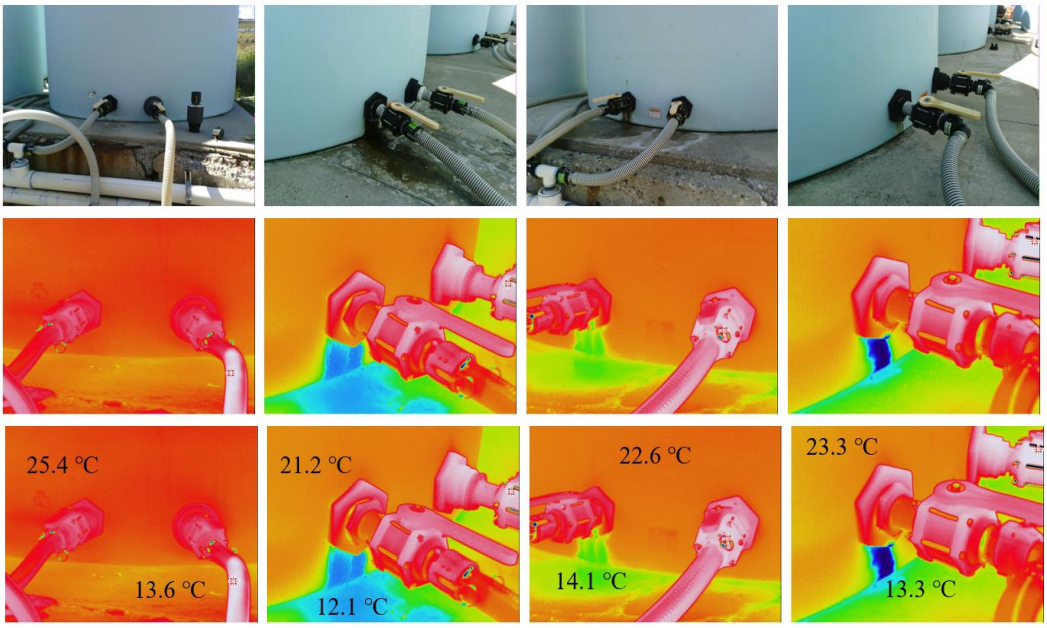

Figure 4-10 Four brine tanks with previous water leakages.

4.4 Summary

In this chapter, we developed and deployed a long-term monitoring system at the UDOT Parley Springs Maintenance Shed over a four-week period in the summer of 2022. The collected thermal images were analyzed, and no significant temperature anomalies were identified corresponding to water leakages. The optical images were investigated to understand the change in deflections of the tank wall. With a 1-mm sensitivity supported by the system, no significant variations in deflection were identified. Finally, a handheld thermal camera was used for site survey, which is effective for leakage detection.

5.0 CONCLUSIONS

5.1 Summary

A dual-spectrum camera was used to monitor the condition of UDOT brine tanks. Meanwhile, computer vision algorithms perform well in automatic temperature extraction and tank wall deflection, showing great potential in brine tank monitoring and maintenance. Therefore, this project developed a reliable and affordable solution for UDOT brine tank inspection, capable of analyzing collected videos by a dual-spectrum camera to facilitate automatic information collection and assessment of brine tank conditions. However, due to the constraints on costs and logistics, it is recommended to use the low-cost infrared camera for routine brine tank inspection, which is detailed in the "UDOT Brine Tank Inspection Manual" in Appendix A.

The computer vision algorithms were developed through laboratory tests. In the field, we collected videos of optical and thermal images over a four-week period, covering both daytime and nighttime. With images collected from the field, the computer vision algorithms were further developed and implemented for automatic information collection to capture temperature variations and tank wall deflections. The results show that the developed NDE approach can support high-accuracy temperature extraction (over 98% correlation) and 1-mm resolution for tank-wall deflection measurements. The findings of the project are summarized below.

- We developed a system based on a dual-spectrum camera for UDOT brine tank condition assessment, targeting measuring wall thickness reduction and tank wall deflections.
- We tested a low-cost thermal camera to perform wall-thickness variation detection, where thermal images can support sub-mm wall-thickness variation detection in a laboratory environment.
- We developed a low-cost brine tank profile evaluation algorithm based on optical images, and the developed algorithm can support sub-mm wall deflection detection in a laboratory environment.

- At UDOT's Parley Springs Maintenance Shed, our temperature extraction algorithm can support 98% correlation with the actual temperature measurements. No significant wall-thinning was identified through our monitoring on 4 brine tanks.
- At the field site, no significant wall deflection variations (>1 mm) were identified through our inspection on brine tanks by comparing two cases with a temperature difference of 30℃.
- Our site survey suggests that thermal images can easily detect brine tank leakages (even without active water leakage) with a temperature difference of 10℃.
- We recommend that UDOT use the developed "UDOT Brine Tank Inspection Manual" as attached in Appendix A.

5.2 Limitations and Challenges

With decent performance in current computer vision algorithm development, limitations still exist, mostly on the tank-wall deflection measurement. Firstly, the edge detection algorithms generally require a clear boundary to achieve a reasonable accuracy, which shall be taken care of at the measurement stage. Secondly, the use of low-resolution cameras can pose a challenge in accurate deflection measurements. Although we tested the approaches at a UDOT site, the performance of the developed algorithms needs to be further evaluated on tanks with active leakage(s).

Considering these limitations, future studies shall explore the relationship between temperature variation and water tank deflection over the years, which can further expand knowledge in this area. The results of this study can serve as a foundation for developing novel techniques and methods for nondestructive evaluation and infrastructure health monitoring. Overall, the project provides valuable insights into the potential of image processing and OCR techniques for infrastructure health monitoring and lays the groundwork for further research in this field.

REFERENCES

Amiri, M., and Sabbagh-Yazdi. S. R. (2011). “Ambient vibration test and finite element modeling of tall liquid storage tanks.” *Thin-Walled Structures*, 49 (8): 974–983.

Batista-Abreu, J. C., and Godoy, L. A. (2013). “Thermal Buckling Behavior of Open Cylindrical Oil Storage Tanks under Fire.” *Journal of Performance of Constructed Facilities*, 27 (1): 89–97. American Society of Civil Engineers (ASCE). https://doi.org/10.1061/(asce)cf.1943-5509.0000309.

Behravan, A., DeJong, M. M., and Brand, A. S. (2021) “Laboratory Study on Nondestructive Evaluation of Polyethylene Liquid Storage Tanks by Thermographic and Ultrasonic Methods.” *Civil Eng*, 2 (4): 823–851. MDPI. https://doi.org/10.3390/civileng2040045.

Bhadauria, S.S. and Gupta, D.M.C. (2007) “In Situ Performance Testing of Deteriorating Water Tanks for Durability Assessment.”, Journal of performance of constructed facilities, 21(3), pp. 234-239. https://doi.org/10.1061/ASCE0887-3828200721:3234.

Gang, D., Shijiu, J., Congying, Z., Weikui, W. (2010). “A study on acoustic emission technology for tank bottom corrosion inspection.” *Anti-Corrosion Methods and Materials*, 1109.

Giergiel, M. et al. (2012). "The project of tank inspection robot." *Key Engineering Materials*. Vol. 518.

Hein, N. W., and Loudermilk, M. D. (1992). “Review of New API-Recommended Practices for Petroleum Production Above Ground Storage Tank Installation, Inspection, and Repair.” *SPE Annual Technical Conference and Exhibition*.

Hodaei, E., Javadi, M., Broumandnia, A., Sadeghi, H. (2012). “Evaluation of acoustic emission inspection of oil tank floor via tank bottom plates thickness measurement.” *Journal of Mechanical Research and Application*, 4(3), pp.37-44.

Kalra, L.P., Gu, J., Meng, M. (2006). “A wall climbing robot for oil tank inspection.” *IEEE International Conference on Robotics and Biomimetics*, pp. 1523-1528.

Lin, M., Kang, Y., Wang, W., Zhang, L., Sun, Y. (2010). “Research on acoustic emission in-service inspection for large above-ground storage tank floors.” *International Pipeline Conference*, Vol. 44229, pp. 233-239.

Liying, S., Yibo, L. (2011). “Investigation on sensor array in large vertical storage tank bottom inspection using AE methods.” *2011 Chinese Control and Decision Conference (CCDC)*, pp. 2838-2842.

Longo, D., Muscato, G. (2004). “A modular approach for the design of the Alicia3 climbing robot for industrial inspection.” *Industrial Robot: An International Journal*.

Lowe, P. S. et al. (2017) “Structural health monitoring of above-ground storage tank floors by ultrasonic guided wave excitation on the tank wall.” *Sensors*, 17.11, 2542.

Mejía, J.A., Hay, J., Mustafa, V., Santa Fé, J. (2010). “Aboveground storage tank floor corrosion condition assessment.” *Avances: Investigacion en Ingeniería*, 1(12):9-13.

Mishra, M., Lourenço, P. B., and Ramana, G. V. (2022). “Structural health monitoring of civil engineering structures by using the internet of things: A review.” *Journal of Building Engineering*.

Moniri, M.M., Bamdad, M., Hajizadeh, A. (2015). “A novel mechatronic design of wall climbing robot for steel storage tank inspection.” *16th International Conference on Research and Education in Mechatronics (REM)*, pp. 1-6.

Murakami, S., Homma, K., Koike, T., Yamada, M., Yuyama, S. (2007). “AE Source Location Using Neural Network on AE Evaluation of Floor Conditions in Above-Ground Tank.” *Journal of Solid Mechanics and Materials Engineering*, 1(7):919-30.

Pan, P., Xing, C., Bai, J., Yu, S., Xu, Y., Zhou, J. and Yu, J. (2022). “A remote deflection detection method for long-span bridges using adaptive mask and high-resolution camera.” *Measurement*, 201. https://doi.org/10.1016/j.measurement.2022.111774.

Puchot, A. R., et al. (2014). “Inspection technique for above ground storage tank floors using MsS technology.” *AIP Conference Proceedings*. Vol. 1581. No. 1.

Schempf, H., Chemel, B., Everett, N. (1995). “Neptune: above-ground storage tank inspection robot system.” *IEEE Robotics & Automation Magazine*, 2(2):9-15.

Taufiq Rochman, S. (2021). “State of the art of tank structural evaluation review: a case study of an elevated concrete water tank concerning crack initiation.’ *Journal of Southwest Jiaotong University*, 56 (5): 90–106. https://doi.org/10.35741/issn.0258-2724.56.5.9.

APPENDIX A: UDOT BRINE TANK INSPECTION MANUAL

(January 2024: This final draft version of the manual was recommended by Dr. Xuan Zhu's University of Utah research team to be considered for use by UDOT in brine tank inspections.)

UDOT manages statewide above-ground storage tanks to store brine as deicing chemicals for the winter maintenance program. The polyethylene storage tanks will age under UV light, become brittle with low temperatures, creep, and develop cracks. Structural failures of brine tanks will not only impose safety hazards to surrounding tanks and UDOT personnel but could also contaminate groundwater. While these tanks are routinely inspected to identify signs of aging and damage, current methods are limited to visual inspection, which may not adequately capture wall thinning. Therefore, it is essential to develop guidelines as an implementable solution for UDOT's routine inspection. This inspection manual solely focuses on visual inspection and the use of low-cost thermal cameras. This document is organized as follows. In Section A.1, we will detail a checklist for external tank inspection. In Section A.2, we will cover the use of a thermal camera for existing and active leakage detection.

A.1 Checklist for External Tank Visual Inspection

This checklist is adopted and modified based on the work of Hein and Loudermilk (1992). It is recommended to perform visual inspection every year and keep documentation.

First, the following information shall be documented to identify the tank under inspection:

Identification

- Tank Designation
- Size
- Date of Inspection
- Measured or Estimated Liquid Level

Second, the condition of the support foundation shall be carefully inspected.

Foundation

- Tank floor level (no differential settlement) Yes/No
- Signs of foundation/soil failure (tank settlement) Yes/No
- Adequate drainage away from tank Yes/No

Third, the condition of the tank bottom shall be carefully inspected.

Tank Bottom

- Visible signs of leakage around tank bottom Yes/No
- Bottom/shell connection free of cracks and leaks Yes/No
- Hosepipe connection free of cracks and leaks Yes/No

Finally, the condition of the tank shell shall be carefully inspected.

Tank Shell

- Tank shell abnormalities/distortions. Yes/No
    - If yes, please describe the condition (number and location).

A.2 External Tank Inspection Using Low-Cost Thermal Camera

It is recommended to perform inspection using a low-cost thermal camera every year during July or August, and keep documentation at times when there will be sufficient heat diffusion through the natural heating-cooling cycles. It is also recommended to perform the inspection using low-cost thermal cameras within the time windows of 10 a.m. to 12 p.m. and from 3 to 6 p.m., when the tank surface temperature ascends to or descends from the peak temperature of the day. Cloudy/windy/rainy days shall be avoided for taking measurements. The

inspector shall always perform auto scaling and auto focusing prior to measurements. A simple trick is to place the finger close to but not touching the surface under inspection and perform the auto focusing.

A low-cost thermal camera, such as the FLIR ONE Pro or a similar product, is suitable for the designated tasks. The FLIR ONE Pro camera offers 4 times the native resolution of the FLIR ONE Pro LT, for sharper image clarity that's further enhanced by the revolutionary FLIR VividIR™. Measured temperatures can go up to 400°C (752°F) with a sensitivity that detects temperature differences down to 70 mK. The FLIR ONE Pro camera can be attached to a personal iPhone or Android phone for data collection, as shown in Figure A-1. This specific model will not be compatible with iPhone 15 and later models. There is a new model, FLIR ONE Edge Pro, with a similar price tag, which can wirelessly connect to and clip thermal images onto smart devices.

The following items shall be incorporated together with the checklist in the previous section.

Tank Bottom

- Visible signs of leakage around tank bottom via thermal camera Yes/No
- Bottom/shell connection free of cracks and leaks via thermal camera Yes/No
- Hosepipe connection free of cracks and leaks via thermal camera Yes/No
    - If no, are those active or previous leakages?
- Please document the thermal images.

Note: Water marks and active leakages can be easily highlighted with up to tens of °C temperature difference measured by the thermal camera, which is caused by drastically different emissivity values on different surfaces.

Tank Shell

- Tank shell temperature abnormalities Yes/No

- If yes, please describe the condition (difference in temperature, overlay with visual abnormalities?).

Figure A-1 FLIR ONE Pro camera attached to an iPhone for data collection.